Journal of Materials Chemistry A

ARTICLE

"Water-in-Salt" electrolyte enables green and safe Li-ion batteries for large scale electric energy storage applications

Liumin Suo,[a] Fudong Han,[a] Xiulin Fan,[a] Huili Liu,[a] Kang Xu* and Chunsheng Wang*

Although state-of-the-art Li-ion batteries have overwhelmed the market of portable electronics as the sole power source, their intrinsic limitations imposed by concerns over their safety, toxicity and cost have prevented them to be readily adopted by large-scale electric energy storage applications. Leveraging the new class of aqueous electrolytes of wide electrochemical stability window to resolve these concerns, we describe a new aqueous Li-ion chemistry based on LiFePO4/Water-in-Salt/Mo_6S_8 that is safe, green and economical. These merits, along with superior electrochemical performances such as excellent cycling stability (>1000 cycles), both high coulombic and round-trip efficiencies, high rate capability, low self-discharge rate at fully charged state, as well as wide service temperature range (-20 ~ +55 ^{o}C), make this new battery chemistry a promising candidate as energy storage unit for large-scale applications.

Introduction,

As energy storage units, the rechargeable batteries are indispensable components in almost any power systems, from vehicle electrification to smart grids that harvest energy from intermittent sources such as solar, wave or wind.[1-3] As battery chemistry of the highest energy density, Li-ion batteries have been considered as primary candidates for such applications; however, their intrinsic limitations arising from the safety, environmental impact and cost have prevented them to be readily adopted in those large-scale applications (1000 ~1,000,000 Wh). Closer examination reveals that most of these concerns originated from the non-aqueous electrolytes used in the state-of-the-art Li-ion batteries. Based on lithium salts containing labile phosphorus-fluorine bonds dissolved in organic carbonate esters, these electrolytes are inflammable, toxic especially when the battery experience thermal runaway,[4] and incur high cost not only directly from the manufacturing, processing and transportation processes of these moisture-sensitive materials, but to an even greater degree from the packaging and safety management of large battery modules and packs.[5-7]

Replacing the non-aqueous electrolytes with an aqueous alternative would resolve all these concerns;[8-12] however, the narrow electrochemical stability window of aqueous electrolytes (< 1.5 V), often defined by the evolution of hydrogen at negative electrode and oxygen at positive electrode surfaces, prevented the use of most Li-ion electrochemical couples, which usually generate a cell voltage of >3.0 V. Such intrinsic limitation, imposed by the potentials where water decomposes into hydrogen and oxygen, constitutes the major obstacle to any attempts of fabricating an aqueous Li-ion battery of high voltage (> 2.0 V) and energy density (> 50 Wh/Kg).[13-19] Even when operating under 1.5 V, most of these systems are still plagued by high self-discharge rates and poor storage stabilities, as revealed by the fact that in literature the aqueous batteries were often cycled at high rates to camouflage the effect of parasitic reactions on cycling stability.

Recently, a new class of aqueous electrolytes was reported by Suo et al, who managed to form solid-electrolyte-interphase (SEI) for the first time in the aqueous media by manipulating the structure of Li^+-solvation sheath.[20] The presence of such aqueous SEI successfully expanded the electrochemical stability window of aqueous electrolytes from ~1.23 V to nearly 3.0 V, thus enabling many Li-ion chemistries that are otherwise impossible. A 2.3 V full Li-ion cell using the electrochemical couple of $LiMn_2O_4$/Mo_6S_8 was demonstrated in such electrolyte, delivering over 1000 cycles at a projected energy density of ~100 Wh/Kg.[20] However, the positive selected therein ($LiMn_2O_4$) is known for its persisting fading behavior in non-aqueous electrolyte, which occurred at least partially via the so-called Jahn-Teller effect arising from the thermodynamic instability of the spinel lattice. This degradation process would accelerate at elevated temperatures (55°C).[21, 22] To seek a more electrochemically stable positive electrode that targets the grid-storage applications, where safety, environmental and cost concerns far outweigh the gravimetric or volumetric energy densities,

a. Department of Chemical and Biomolecular Engineering, University of Maryland College Park, Maryland, 20740, USA.
E-mail: cswang@umd.edu
b. Electrochemistry Branch, Sensor and Electron Devices Directorate, Power and Energy Division U.S. Army Research Laboratory Adelphi, Maryland, 20783, USA
E-mail: conrad.k.xu.civ@mail.mil
† Footnotes relating to the title and/or authors should appear here.
Electronic Supplementary Information (ESI) available: [details of any supplementary information available should be included here]. See DOI: 10.1039/x0xx00000x

we turned our attention to LiFePO$_4$. The olivine lattice structure of this positive material has been known for its thermal stability, non-toxicity, safety and low cost.[23, 24] Previously, LiFePO$_4$ has been used in aqueous electrolytes due to its moderate lithiation/de-lithiation potential (3.5 V vs. Li).[25-27] However, on one hand, in the alkaline electrolyte and in the presence of dissolved oxygen, LiFePO$_4$ became unstable during charging;[28] on the other, re

stricted by the narrow electrochemical stability window of aqueous electrolyte and the consequent limited choice of anode materials, the output voltage of aqueous Li-ion full cells using LiFePO$_4$ is constantly less than 1.0 V, making the benefits of such aqueous alternatives marginal.[15] With ability to form SEI in aqueous media, the new "Water-in-Salt" electrolyte significantly relaxed the cathodic restrictions from 2.6V to 1.9V (vs. Li), hence allowing the use of anode materials with redox potentials below 2.6 V, such as cheval phase Mo$_6$S$_8$. Furthermore, the neutral (pH ~7.0), resistance against oxygen dissolution, non-corrosive and ambient-insensitive nature of the new electrolyte not only ensured the reversibility of LiFePO$_4$ but also introduced additional packaging and environmental benefits to the manufacturing and processing of the cells and materials. The combination of electrochemical coupling LiFePO$_4$, Mo$_6$S$_8$ and "Water-in-Salt" electrolyte would lead to a full Li-ion cell chemistry of 1.3V with expected merits arising from all three materials: the non-toxicity, high safety, excellent cycling and thermal stability, high coulombic and round-trip efficiencies, wide service temperature range, high rate capability as well as storage stability. These advantages would undoubtedly result in a system that best suits the key requirements of large scale energy storage units.

Experimental

Materials

The chevrel phase Mo$_6$S$_8$ was prepared by leaching Cu from copper chevrel powder CuMo$_3$S$_4$ that was synthesized via solid-state synthesis. CuS (99% Sigma-Aldrich), Mo (99.99% Sigma-Aldrich), MoS$_2$ (99% Sigma-Aldrich) were grounded by ball-milling for 0.5h, then the powder was pelleted at 10MPa and sealed in a stainless steel Swagelok cell, which were heated to 900 °C for 24h with heating rate of 2 °C/min in Argon. The products were placed and stirred in a 6 M HCl solution for 12 h with O$_2$ bubbling to remove Cu. Finally, the obtained chevrel powder (Mo$_6$S$_8$) was washed with deionized water for three times under vacuum filtration followed by drying at 100 °C overnight. The LiFePO$_4$ was purchased from A123 Corporation.

Materials Characterization

X-ray diffraction patterns were recorded on D8 Advance X-ray diffraction (Bruker), with Cu Kr radiation in the 2-theta range of 10~90 degree. Scanning electron microscopy (SEM) was conducted on a Hitachi S-4700 (Japan) operating at 10 kV, and transmission electron microscopy (TEM) on a Hitachi S-4700

(Japan) operating at 10 kV and in a JEOL (Japan) 2100F field emission, respectively. X-ray photoelectron spectroscopy (XPS) analysis was performed on a high resolution Kratos AXIS 165 X-ray photoelectron spectrometer using monochromic AlKa radiation.

Electrochemical Measurements

The electrodes were fabricated by compressing active materials, carbon black, poly(vinylidene difluoride) (PTFE) at the weight ratios of 8:1:1 on a stainless steel grid before electrochemical performance measurement. The aqueous "Water-in-Salt" electrolyte was made by dissolving 21m lithium bis(trifluoromethane sulfonyl)imide (LiTFSI) in de-ionized H$_2$O. Cyclic voltammetry (CV) was carried out using CHI 600E electrochemical work station and three-electrode cells. The CV of LiFePO$_4$ was conducted with LiFePO$_4$ as working, excessive active black (AB) as counter and Ag/AgCl as reference electrodes, respectively. The CV of Mo$_6$S$_8$ was conducted with Mo$_6$S$_8$ as working electrode, a 2 mm platinum dish as counter and Ag/AgCl as reference electrodes. The potentials refering to Ag/AgCl reference electrode were converted to Li$^+$/Li for convenience. CV was also applied to determinate the electrochemical stability window of electrolytes using electrochemically inert electrodes (316 stainless steel grid, 200-mesh sieve) as working and counter
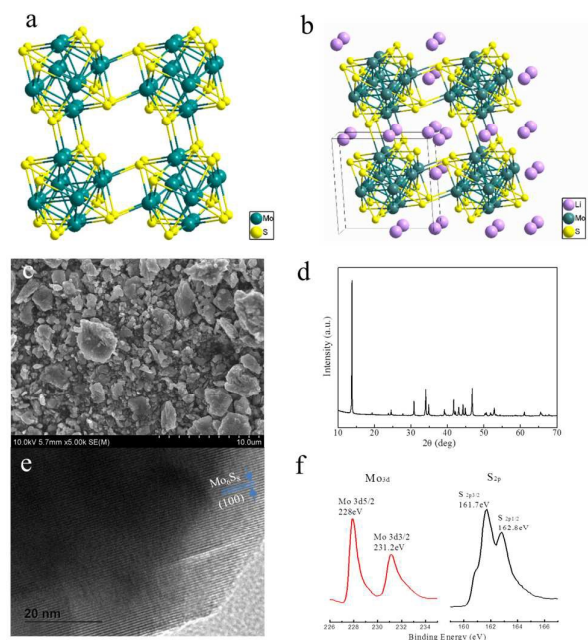

Fig. 1. The chevrel phase Mo$_6$S$_8$. (a), (b) the crystal structures of Mo$_6$S$_8$ and Li$_4$Mo$_6$S$_8$, (c), (d) SEM and high solution TEM image of pristine Mo$_6$S$_8$, (e) X-ray pattern of Mo$_6$S$_8$ and (f) XPS spectra of Mo$_6$S$_8$.

electrodes. They were thoroughly cleaned with high purity alcohol under ultrasonic agitation, followed by washing with high purity water for three times and then drying before measurements. The full Li-ion cells were assembled in CR2032-

type coin cell configuration with the $LiFePO_4$ as positive, Mo_6S_8 as negative electrode and a glass fiber as separator. The active mass ratio of $LiFePO_4$ to Mo_6S_8 was set to be 2:1. The galvanostatic cycling was carried out on a Land BT2000 battery test system (Wuhan, China) at room-temperature (25 ^{o}C).

Results and discussion

The excellent cycling stability of $LiFePO_4$ in both non-aqueous and aqueous electrolytes has been reported in previous literature.[15, 29] In this work we selected a commercial $LiFePO_4$ materials from A123, whose XRD and SEM images were shown in Figure S1 and S2, respectively. The crystal structure and morphology of Mo_6S_8 at either pristine (Mo_6S_8) or fully-lithiated ($Li_4Mo_6S_8$) states were shown in Figure 1. Apparently the Mo_6S_8 unit can be considered as an octahedron of Mo atoms in a cube of S atoms, and chevrel phase arranges by the Mo_6S_8 clusters tilted relatively to each other, in which a large number of sites exist among clusters that constitutes diffusion channels for ion transport. Thus, chevrel phase Mo_6S_8 has high

Fig. 2. Cycling voltammetry (CV) of the electrodes and electrolyte materials. (a) The electrochemical stability window of Water-in-Salt electrolyte as measured on inert current collector (stainless steel grid) at scanning rate of 10 mV/s, which is overlaid with the 1st CV traces of active anode (Mo_6S_8) and positive ($LiFePO_4$) materials measured at scanning rate of 0.1 mV/s in the same electrolyte, (b) the evolution of CV traces of chevrel phase Mo_6S_8 and (c) olivine $LiFePO_4$ at scanning rate of 0.1 mV/s.

electronic and ionic conductivities, making it a suitable electrode for both Li^+ and Mg^{2+} intercalations.[30, 31] The XRD pattern in Figure 1d reveals the Mo_6S_8 sample as pure chevrel phase (space group: R-3 and JCPDS-ICDD: 00-027-0319) after the as-prepared $Cu_2Mo_6S_8$ was etched by HCl. To confirm the chevrel phase, surface chemistry of Mo_6S_8 was investigated by XPS (Figure 1f). The characteristic twin peaks for both Mo and S shell electrons (Mo_{3d} and S_{2p}) are identified at the expected binding energies ($Mo_{3d5/2}$~228eV, $Mo_{3d3/2}$~231.2eV and $S_{2P3/2}$~161.7 eV, $S_{2P1/2}$~162.8 eV).

A three-electrode cell was used to evaluate the compatibility and reversibility of $LiFePO_4$ or Mo_6S_8 in the concentrated aqueous electrolyte. As Figure 2a shows, the expanded electrochemical window of the novel aqueous electrolyte is sufficiently wide to support the electrochemical couple of $LiFePO_4$ and Mo_6S_8. As described in our earlier report, the increased Li^+-activity due to the high LITFSI concentration shifts the redox potentials positively, but the potential difference between positive electrode and negative electrode (i.e., the cell voltage) remains constant at all salt concentrations. The evolution of CV for Mo_6S_8 and $LiFePO_4$ are shown in Figures 2b and c, verifying the high reversibility of these electrode materials. In particular (Figure 2b), Mo_6S_8 shows nearly zero fading within 100 cycles by CV at slow scanning rate (0.1mV/s), with the exception of the 1st cycle where part of the irreversible lithium consumption was caused by SEI formation. Since the redox potential of this negative electrode lies beyond the hydrogen evolution potential of salt-in-water aqueous electrolyte at neutral condition (2.63 V vs. Li), this stability highlights the excellent protective effect of the formed SEI.
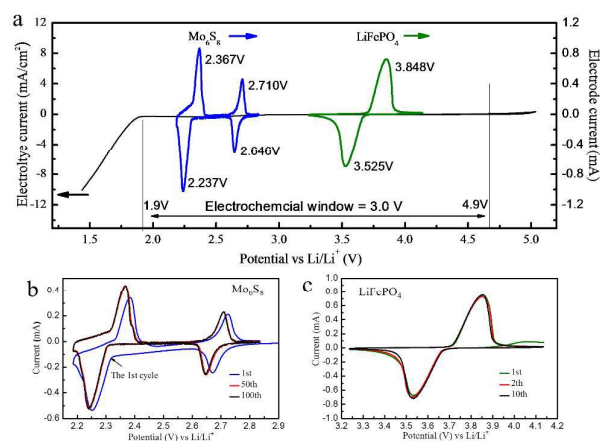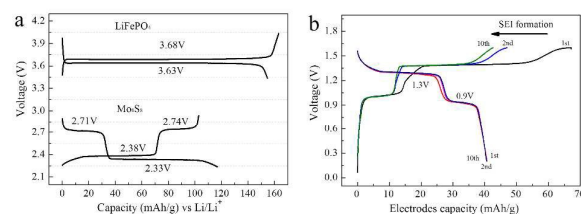

Fig. 3. The charge-discharge profiles. **(a)** The typical voltage profiles of $LiFePO_4$ and Mo_6S_8 electrodes in three-electrode devices at constant current (0.2 C) and **(b)** The voltage profiles of full-cell configuration ($LiFePO_4/Mo_6S_8$) at constant current (0.2 C).

The performance of this electrochemical couple was further evaluated in the same three-electrode cells, in which negative electrode and positive electrode were subject to constant current cycling at different rates in the presence of an independent Ag/AgCl reference electrode (Figure 3). In this manner both voltage of the full cell as well as potentials of individual electrodes (relative to Li^+/Li) can be monitored simultaneously. To evaluate how stable the electrolyte is in contact with these electrodes, both low and high rates (0.20 C and 1 C) were used. As Figure 3a shows, $LiFePO_4$ presents one plateau (charge: 3.69 V and discharge: 3.64 V) and Mo_6S_8 display two plateaus (charge: 2.38 V and 2.74 V and discharge: 2.71 V and 2.33 V), which consequently leads to two distinct discharge plateaus for the full cell at 1.3 V and 0.9 V (Figure 3b). To compensate for the irreversible loss caused by SEI formation, we set the ratio of $LFePO_4$ to Mo_6S_8 to be 2:1 by weight. The electrochemical performance of $LiFePO_4/Mo_6S_8$ full cell was tested in coin cells and shown in Fig. 4. As shown in Fig. 4a, the formation process of SEI should complete within 10 cycles, after which a Coulombic efficiency above 96% was achieved at 0.20 C. Considering that the negative actually operates at a potential below that of hydrogen evolution, this

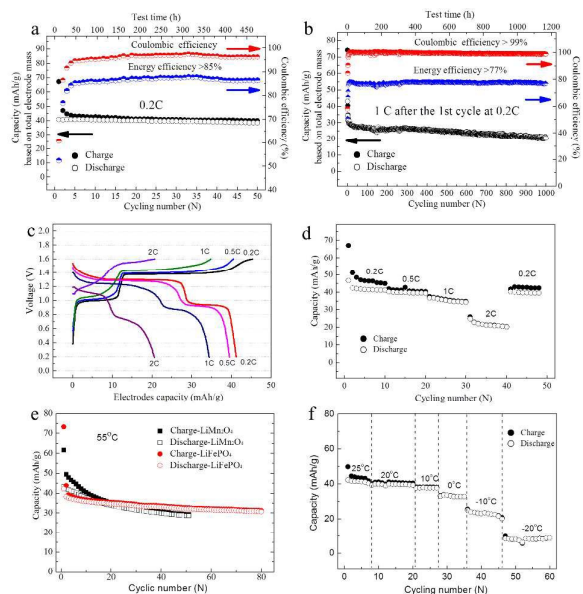high Coulombic efficiency achieved at this low rate is

Fig. 4. Electrochemical performances of full Li-ion cell based on LiFePO$_4$/Mo$_6$S$_8$. (a) and (b) the cycling stability, round trip energy efficiencies and Coulombic efficiencies of full Li-ion cell at low (0.2 C) and high (1 C) rates respectively; (c) and (d) the rate capability at room temperature; (e) The comparison of elevated temperature cycling stability (55°C) between LiFePO$_4$ and LiMn$_2$O$_4$; (f) low temperature cycling stability from 25°C to -20°C. All the capacity shown in Fig 4 is calculated based on the total electrode masses of LiFePO$_4$ and Mo$_6$S$_8$.

unprecedented.

Based on the first discharge data normalized by the total mass of both positive and negative electrodes, the full Li-ion cell delivers an energy density of 47 Wh/Kg. The charge/discharge efficiencies at 0.2C and 1C, calculated by the energy the full cell absorbs and releases, are also plotted in Figure 4a and 4b. It shows high round-trip efficiencies with > 85% at 0.2C and >77% at 1C respectively. At low rate (0.2C), after 50 cycles and above 20 days of testing time, the full Li-ion cells still retain 94.3% of the initial capacity (the first discharge: 40.7 mAh/g and the 50th discharge: 38.4 mAh/g). At high rate (1C), cycling life readily lasts over 1000 cycles (the testing time: about 49 days) with the low fading rate of 0.04% per cycle and high coulombic efficiency above 99%. Although 21 m of LiTFSI was added into water, the the Li-ion conductivity of the Water-in-Salt electrolyte is still higher than 10^{-2} S cm^{-1},[12] allowing high rate performance as demonstrated in Fig. 4c & d. The electrochemical performances were also evaluated under different temperatures that the Nature could impose to large-scale grid-storage system, from +55 ^{o}C down to -20 ^{o}C (Figure 4 e and f). Apparently, at 55°C the LiFePO$_4$/Mo$_6$S$_8$ full cell outperformed LiMn$_2$O$_4$/Mo$_6$S$_8$ in cycling stability, while the latter demonstrated a rapid capacity fading, the reason

underneath which might be the well-known Jahn-Teller transformation and subsequent Mn dissolution accelerated by the high temperature (55°C). On the other hand, with the temperature decreasing from 25°C into -20°C stepwise (Fig. 4d), the delivered capacity of full Li-ion cell decreased accordingly; however, even at -20°C, the cell still cycles as evidenced by the voltage profiles shown in Figure S3.

It has been widely believed that long cycling life is difficult to achieve for aqueous Li-ion batteries, especially at rates lower than 1C, even when the operating potential of negative materials lies within the thermodynamic stability of water (< 1.5 V). The rationale for this instability originates from the fact the hydrogen evolution occurs at fast kinetics that cannot be readily delayed. In literature describing the cycling behavior of aqueous Li-ion cells, high rates (> 1 C) were almost exclusively
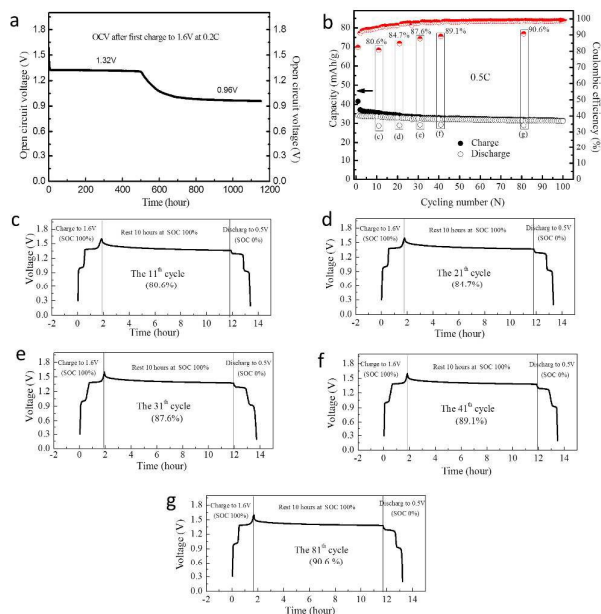

Fig. 5. Electrochemical storage of full cell based on LiFePO$_4$/Mo$_6$S$_8$. (a) The OCV decay at fully charged state of 1.6 V at 0.2C, (b) The cycling performances at 0.5C with a 10-hour rest at every 10 or 50 cycles. The self-discharge was evaluated by comparison with the columbic efficiency and the capacity loss after resting. (c) ~ (g), the voltage profiles of charging and discharging immediately before and after the 10-hour rest.

used in order to minimize the effect of hydrogen evolution on capacity retention. Such tactical approaches, however, could be misleading, because as Dahn and coworkers demonstrated that the real stability does not come from number of cycles but from the duration that a system stays at fully charged state, or from the Coulombic efficiencies observed at low cycling rates.

In this context, the superior cycling stability demonstrated at 0.20 C in our work using a negative electrode that operates beyond the hydrogen evolution potential underlines the effectiveness of the formed SEI. One primary mission for large-scale grid-storage batteries is how well the harvested energy could be kept at the fully charged state (100% state-of-charge,

or SOC) during the storage phase. In order to evaluate the storage performance of aqueous LiFePO$_4$/Mo$_6$S$_8$ full cell, we employed two different approaches. We first monitored the decay of open circuit voltage (OCV) at 100% OCV (Figure 5a), because the negative electrode at fully lithiated state is most electrochemically active, and most of the parasitic reactions occurring thereon could be the source of self-discharge. Fig. 5a shows negligible potential change, which remains above 1.32 V after 20 days, and then it drops to 0.96V. In the worst case, if we assume that all capacity loss during this storage period is entirely incurred by the parasitic reactions at Mo$_6$S$_8$ anode side alone, and that the theoretical capacity of Mo$_6$S$_8$ anode in the first discharge plateau is about 85 mAh/g (128mAh/g × 2/3 = 85mAh/g) (Figure 3 a), then the self-discharge rate of the full Li-ion cell is estimated to be less than 0.13 % per hour at 100% SOC, which is the lowest in all reported aqueous rechargeable Li-ion systems so far. Since this data is obtained from non-optimized coin cells fabricated in laboratory, experience tells us that there is much space for further improvement via cell design and engineering. The low self-discharge rate of LiFePO$_4$/Mo$_6$S$_8$ full cell at beyond the hydrogen evolution potential is attributed to the protection by the formed SEI. Secondly, we attempted to correlate SEI formation with self-discharge rate. We cycle the cell continuously and then place it on a 10-hour rest at 100% SOC every 10 cycles, before cycling resumes. The capacity loss between charge and discharge cycles after the 10-hour rest could reveal any self-discharge behavior of the full Li-ion cell (Figure 5b). As shown by Figure 5b, the Coulombic efficiencies among the cycles interrupted by rest steadily increases with cycle number, e.g., 80.6% at the 11th cycle: 84.7% at the 21th cycle, 87.6% at the 31th cycle, and 89.1% at the 41th cycle. We believe that the trend of Coulombic efficiency actually reflects the gradual formation process of SEI at anode, which becomes more and more effective in protecting the anode surface against parasitic hydrogen evolution reactions. The voltage profiles of the charging and discharging processes immediate before or after each 10-hour rest (Figure 5 c~g) clearly reveal this evolution process which stabilizes after 80 cycles with above 90% coulombic efficiency after resting 10 hours at 100% SOC. By this time, we believe that SEI formation is almost completed. Overall, SEI formation is determined by both charge-discharge time and cycles. Thus, as Figure 4b shows, the batteries could be first formed at low rate (0.2C) during the initial cycles, and then subject to high rates. In this case, nearly 100% Coulombic efficiency could be achieved after 10 cycles, which indicates the maturing of the system for energy storage mission.

Conclusions

In summary, we report a safe, green and low cost aqueous Li-ion battery chemistry that targets the large-scale energy storage applications. The full Li-ion cell based on LiFePO$_4$/"Water-in-Salt" electrolyte/Mo$_6$S$_8$ combines advantages of state-of-the-art Li-ion batteries (long cycling life, high around-trip efficiency and low maintenance) and aqueous

batteries (low production cost, green and high safety). Its superior cycling reversibility (> 1000 cycles) at both low (0.2C) and high (1C) rates with high Coulombic efficiency, along with durability against extreme temperatures from -20 to 55 ^{o}C and excellent storage retention at fully charge state, make it a competitive candidate for the energy-harvesting smart-grid.

Notes and references

1 B. Dunn, H. Kamath and J.-M. Tarascon, *Science*, 2011, **334**, 928-935.
2 Z. Yang, J. Zhang, M. C. W. Kintner-Meyer, X. Lu, D. Choi, J. P. Lemmon and J. Liu, *Chemical Reviews*, 2011, **111**, 3577-3613.
3 H. Pan, Y.-S. Hu and L. Chen, Energy & Environmental Science, 2013, 6, 2338-2360.
4 A. Hammami, N. Raymond and M. Armand, *Nature*, 2003, **424**, 635-636.
5 J. M. Tarascon and M. Armand, *Nature*, 2001, **414**, 359-367.
6 K. Xu, *Chemical Reviews*, 2004, **104**, 4303-4417.
7 K. Xu, *Chemical Reviews*, 2014, **114**, 11503-11618.
8 W. Yang, K. Kang, H. Li, X.-Q. Yang, L. Chen and X. Huang, Nature Communications, 2015, 6.
9 M. Pasta, C. D. Wessells, R. A. Huggins and Y. Cui, Nature Communications, 2012, 3.
10 Y. Wang, J. Yi and Y. Xia, *Advanced Energy Materials*, 2012, **2**, 830-840.
11 C. Wessells, R. A. Huggins and Y. Cui, Journal of Power Sources, 2011, 196, 2884-2888.
12 H. Kim, J. Hong, K.-Y. Park, H. Kim, S.-W. Kim and K. Kang, Chemical Reviews, 2014, 114, 11788-11827.
13 W. Li, J. R. Dahn and D. S. Wainwright, *Science*, 1994, **264**, 1115-1118.
14 W. Tang, Y. Zhu, Y. Hou, L. Liu, Y. Wu, K. P. Loh, H. Zhang and K. Zhu, *Energy & Environmental Science*, 2013, **6**, 2093-2104.
15 J.-Y. Luo, W.-J. Cui, P. He and Y.-Y. Xia, *Nature Chemistry*, 2010, **2**, 760-765.
16 C. Wessells, R. Ruffo, R. A. Huggins and Y. Cui, Electrochemical and Solid State Letters, 2010, 13, A59-A61.
17 R. Ruffo, C. Wessells, R. A. Huggins and Y. Cui, Electrochemistry Communications, 2009, 11, 247-249.
18 Q. T. Qu, L. J. Fu, X. Y. Zhan, D. Samuelis, J. Maier, L. Li, S. Tian, Z. H. Li and Y. P. Wu, Energy & Environmental Science, 2011, 4, 3985-3990.
19 W. Tang, L. L. Liu, Y. S. Zhu, H. Sun, Y. P. Wu and K. Zhu, Energy & Environmental Science, 2012, 5, 6909-6913.
20 L. Suo, O. Borodin, T. Gao, M. Olguin, J. Ho, X. Fan, C. Luo, C. Wang, K. Xu, *Science*, 2015, **350**, 938-943
21 D. H. Jang, Y. J. Shin and S. M. Oh, *Journal of the Electrochemical Society*, 1996, **143**, 2204-2211.
22 Y. Y. Xia, Y. H. Zhou and M. Yoshio, *Journal of the Electrochemical Society*, 1997, **144**, 2593-2600.
23 D. Choi, D. Wang, V. V. Viswanathan, I.-T. Bae, W. Wang, Z. Nie, J.-G. Zhang, G. L. Graff, J. Liu, Z. Yang and T. Duong, *Electrochemistry Communications*, 2010, **12**, 378-381.
24 X.-L. Wu, L.-Y. Jiang, F.-F. Cao, Y.-G. Guo and L.-J. Wan, *Advanced Materials*, 2009, **21**, 2710-+.

25 C. H. Mi, X. G. Zhang and H. L. Li, *Journal of Electroanalytical Chemistry*, 2007, **602**, 245-254.
26 Y. Hou, X. Wang, Y. Zhu, C. Hu, Z. Chang, Y. Wu and R. Holze, *Journal of Materials Chemistry A*, 2013, **1**, 14713-14718.
27 P. He, X. Zhang, Y.-G. Wang, L. Cheng and Y.-Y. Xia, *Journal of the Electrochemical Society*, 2008, **155**, A144-A150.
28 M. Minakshi, S. Pritam, T. Stephen, P. Kathryn, *Journal of Power Sources*, 2006, **158**, 646-649.
29 M. Takahashi, H. Ohtsuka, K. Akuto and Y. Sakurai, *Journal of the Electrochemical Society*, 2005, **152**, A899-A904.
30 P. J. Mulhern and R. R. Haering, *Canadian Journal of Physics*, 1984, **62**, 527-531.
31 D. Aurbach, Z. Lu, A. Schechter, Y. Gofer, H. Gizbar, R. Turgeman, Y. Cohen, M. Moshkovich and E. Levi, *Nature*, 2000, **407**, 724-727. Y. Wang, J. Liu, B. Lee, R. Qiao, Z. Yang, S. Xu, X. Yu, L. Gu, Y.-S. Hu,

Table of Content
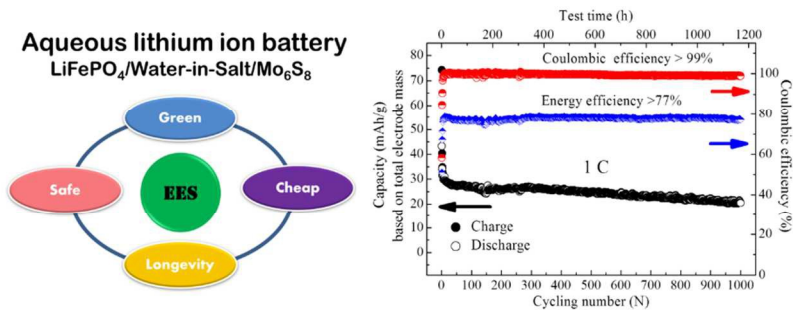
One sentence:

A new, safe, green and economical aqueous Li-ion chemistry based on LiFePO$_4$/Water-in-Salt/Mo$_6$S$_8$ was designed targetedly for large-scale energy electric storage (EES) applications.